NUMERICAL COMPUTATION OF VISCOUS FLOWS ON THE LEE SIDE OF BLUNT SHAPES FLYING AT SUPERSONIC SPEEDS

By John V. Rakich

NASA Ames Research Center

and

Stephen C. Lubard

RDA Inc.

SUMMARY

A numerical method for solving the parabolic approximation to the steady-state compressible Navier-Stokes equations is critically examined. The approximation neglects only the streamwise gradients of shear stress. An implicit finite difference method is used which advances the solution downstream from an initial data surface and determines the complete viscous-inviscid flow between the body and bow shock wave. It is necessary that the inviscid portion of the flow field be supersonic. Crossflow separation is also determined as part of the solution.

The method is applied to a 15° sphere-cone at 15° angle of attack, and the results are compared with available experiment and with an inviscid method-of-characteristics calculation. Excellent agreement between viscous and inviscid theories is obtained in the inviscid regions of the flow. The viscous calculations agree well with experimental surface and pitot pressures and with surface heating rates.

INTRODUCTION

The flow field on the leeward side of bodies has received considerable attention for many years. The flow is inherently viscous and develops into a vortex at moderate angles of attack. At high speeds, lee-side flows are important because the local heating is difficult to correlate and because the shed vortices can interact with aircraft components such as a canopy, a vertical tail, etc. Recently, for example, lee-side flows have become a factor in the design of the space shuttle orbiter thermal protection system.

Lee-side flows are difficult to calculate because thin-boundary-layer theory is not applicable and the concept of matching inviscid and viscous flow becomes highly questionable. Early attempts to predict lee-side flows were based on vortex tracing methods. However, for such methods the separation point must be specified, a priori, and that point is unknown. Therefore vortex tracing methods are inherently empirical. Recently, two new approaches have been proposed to study the lee-side flow for a pointed cone. One approach utilizes boundary-layer type equations (Lin and Rubin, ref. 1) and requires that the pressure distribution be specified. The second approach (Lubard and Helliwell, ref. 2) makes use of the parabolic approximation to the compressible Navier-Stokes equations and solves for the complete inviscid and viscous regions of flow, including the pressure.

It is the application of the method of Lubard and Helliwell to blunt-nosed bodies that is the topic of the present paper. To use this method it is necessary to first determine an initial data solution in a region where the inviscid portion of the flow is supersonic. The starting solution for the present paper was obtained with the inviscid blunt body and method-of-characteristics codes of references 3 and 4, together with a boundary-layer program, reference 5. The results obtained for a 15° sphere-cone at 15° angle of attack are compared with experiment and with inviscid theory.

ANALYSIS

The so-called "parabolic Navier-Stokes" equations, and the numerical methods employed to solve them, have been described previously in references 2 and 6. Only the main features will be discussed here in order to illustrate the capabilities and limitations of the method.

The parabolic approximation results from the assumption that the stress derivatives in the streamwise direction are small in comparison with derivatives in the normal and circumferential directions. This assumption permits the calculation of the flow to proceed downstream from an initial data surface, provided the inviscid region of flow is supersonic. The equations have a parabolic character with respect to the downstream direction, and are elliptic with respect to the surface normal and circumferential directions. Separation and reverse flow is permitted in the crossflow plane, provided the component of velocity in the marching direction is positive. This crossflow separation causes a spiral flow pattern and is the initial stage of formation of the vortices which trail a lifting body.

To start the solution, it is necessary to determine an initial data surface in the supersonic part of the inviscid flow. For the present application to a sphere cone, the flow at the sphere-cone juncture is not separated and boundary-layer theory is applicable there. Also, the flow on the sphere is axisymmetric with respect to wind axes, which simplifies the boundary-layer solution. Therefore, an axisymmetric boundary-layer code (ref. 5) was applied along streamlines from the stagnation point to the sphere-cone juncture. The edge conditions and the inviscid part of the shock

layer were calculated with a blunt-body technique (ref. 3) coupled with a three-dimensional characteristics program (ref. 4). An approximate starting solution was then obtained by simply patching the inviscid flow to the outer edge of the boundary layer (see fig. 1). This displaces the inviscid flow a little too much but it proved to be an adequate approximation for the present example.

The numerical method is the same one used by Lubard and Helliwell (ref. 2) for pointed cones, and is similar to the technique developed by Rubin and Lin (ref. 7). It is an implicit finite difference scheme which employs an iterative matrix inversion scheme. The circumferential derivatives are evaluated in terms of known quantities from the previous iteration, and the matrix is inverted sequentially, one ray at a time. The radial and circumferential derivatives are iterated such that the converged value is obtained at the solution point. For example, the second derivative of velocity, u, is approximated by

$$\left(\frac{\partial^2 u}{\partial \Phi^2}\right)^n_{j,k,\ell} = \left[\frac{u^{n-1}_{j,k,\ell+1} - 2u^{n}_{j,k,\ell} + u^{n-1}_{j,k,\ell-1}}{(\Delta\Phi)^2}\right] \tag{1}$$

where j,k,ℓ are mesh indices for the x,η,Φ directions (fig. 2), respectively, and n is the iteration index. A backward difference is used for the streamwise derivatives. For example, the streamwise derivative of momentum, ρu, is approximated by

$$\left(\frac{\partial \rho u}{\partial x}\right)^n_{j,k,\ell} = \left[\frac{(\rho u)^{n}_{j,k,\ell} - (\rho u)^{n}_{j-1,k,\ell}}{\Delta x}\right] \tag{2}$$

The finite difference grid had 19 equally spaced planes circumferentially, and 50 unequally spaced points radially. About half the radial points were positioned in the boundary layer. Figure 2 shows the grid and computing time for the sample case, and compares with those for an inviscid solution. Only 87 marching steps were taken in the implicit viscous calculation as compared with 508 steps in the inviscid characteristics calculation, which is constrained by the Courant-Friedrichs-Lewey (CFL) condition. The viscous calculation required 23 minutes of computing time for 950 points per marching plane, and the inviscid calculation required 6 minutes for 399 points per plane. Note, however, that neither code was run at the absolute maximum step size. Also, the characteristics code is not the most efficient method from the computational point of view. Therefore the comparison in figure 2 should only be considered qualitative. On this basis, and considering the finer resolution, the computer time required by the viscous code is not excessive.

Because of a peculiarity of the parabolic Navier-Stokes approximation, the finite difference method has a lower bound on the marching-step size. If too small a step size is attempted, nonphysical branching solutions can be generated (see ref. 2). The reason for this behavior is discussed by Rubin and Lin in reference 7 where it is pointed out that the equations have a singularity at the sonic line in the boundary layer, and at that point some

upstream influence is allowed. The singularity did not cause any difficulty in the present example.

RESULTS

In order to adequately establish the validity of the described numerical technique, it is essential to compare both with experiment and with other numerical methods. Since other viscous flow methods are not available, comparison is made with an inviscid solution obtained with the method of characteristics (ref. 4). The viscous and inviscid results should agree outside the boundary layer in regions where the boundary layer is thin.

The configuration selected for comparison was a 15° half-angle cone with a sphere nose and at 15° angle of attack. This blunt cone model was tested by Cleary in the Ames 3.5-foot hypersonic wind tunnel at $M = 10.6$ (refs. 8-10). Surface pressures and heating rates, as well as shock-layer pitot-pressure distributions were measured in the experiments. The angle of attack selected was the largest value for which complete test data were available, and was large enough to cause crossflow separation. Complete test conditions are shown in figure 3.

Figure 4 shows the surface-pressure coefficient for three meridional planes. There is reasonably good agreement between both numerical methods (viscous and inviscid) on the windward side $\Phi = 0$, as is expected. Note, however, that on the leeward side the inviscid theory breaks away from the viscous theory at about $x/R_N = 5$. This is approximately the region where a crossflow separation first appears in the viscous flow calculation.

Figures 5 and 6 show the pitot-pressure distributions between the shock and body. Here, η is the distance along the outward normal from the body surface, x is the axial distance from the nose, and R_N is the nose radius. At $x/R_N = 3.4$ the inviscid result seems to agree best with experiment. This is attributed to the way in which the inviscid solution was patched to the boundary layer to obtain an approximate starting solution. The displacement effect is too large, especially on the leeward side. At both stations, $x/R_N = 3.4$ and 14.7, the agreement between inviscid and viscous computations is very good on the windward side. Significant deviations between the two theories occur only near the body where the well-known blunt-body entropy layer and the boundary layer tend to merge.

It should be noted that the model used for the pitot-pressure experiment had a relatively hot wall. It is estimated that the ratio of wall to total temperature could have reached 0.6 for the pressure test as compared to a value of 0.26 for the heating test and for the viscous computations. The higher wall temperature would cause a thicker boundary layer and might explain the difference between the viscous theory and experiment for $\Phi = 0$ and 30° in figure 6(a). For $\Phi = 60°$ and 90°, the experimental pitot pressures are lower than both numerical solutions in the region where viscous effects should be small. This difference is attributed to misalinement of

the pitot probe and flow direction in the experiment.

On the leeward side at $x/R_N = 14.7$, there is excellent agreement between the viscous calculations and experiment, while inviscid calculations overpredict the pressure for the entire shock layer.

The heating rates are compared in figure 7 and the agreement is excellent.

Finally, in figure 8 the crossflow velocity field is shown in the vicinity of the leeward side at $x/R_N = 14.7$. Crossflow separation is indicated at about 22° off the leeward plane of symmetry. Experimental data were not available on the separation-point location for the present test case.

CONCLUDING REMARKS

A marching method for calculating the complete viscous/inviscid flow over blunt bodies at angle of attack has been described and tested for a sphere-cone at moderate angle of attack. It is found to give fairly good agreement with available experiments and is in agreement with inviscid theory where viscous effects are small. The lee-side flow field, including crossflow separation, is predicted without the need for any assumptions about the pressure distribution or the separation point. The present method should be capable of following the vortex initiated by crossflow separation as it sheds and moves away from the body surface. Additional tests of the method are needed to establish this capability. In this regard, it may be necessary to allow lateral asymmetry for the calculation to correctly model vortex shedding.

The computation time for the test case was 23 minutes on a CDC 7600 computer. This is only about four times longer than an inviscid calculation with half as many points. The time per step is an order of magnitude longer than for the inviscid calculation but the implicit finite difference scheme allowed larger marching steps.

The methods described can also be applied to bodies with more general cross-sectional shape, and work is currently progressing along these lines. However, the approximate technique used for the starting solution may not work as well for a general nose shape. For general nose shapes a time-dependent method of solution, such as that described in reference 11, would give a better starting solution.

REFERENCES

1. Lin, T. C., and Rubin, S. G.: Viscous Flow Over a Cone at Incidence, Part 2: Boundary Layer. J. Fluid Mech., vol. 1, July 1975, pp. 593-620.

2. Lubard, S. C., and Helliwell, W. S.: Calculation of the Flow on a Cone at High Angle of Attack. AIAA J., vol. 12, no. 7, July 1974.

3. Moretti, G., and Bleich, G.: Three-Dimensional Flow Around Blunt Bodies. AIAA J., vol. 5, no. 9, 1967.

4. Rakich, John V.: A Method of Characteristics for Steady Three-Dimensional Supersonic Flow with Application to Inclined Bodies of Revolution. NASA TN D-5341, 1969.

5. Bartlett, E. P., and Kendall, R. M.: Nonsimilar Solution of the Multicomponent Laminar Boundary Layer by an Integral Matrix Method. Aerotherm Final Report No. 66-7, Part III, March 13, 1967; also AIAA J., 6, pp. 1089-1097, 1968.

6. Lubard, Stephen C., and Rakich, John V.: Calculation of the Flow on a Blunted Cone at a High Angle of Attack. AIAA paper 75-149, 13th Aerospace Sciences Meeting, Pasadena, Calif., Jan. 20-22, 1975.

7. Rubin, S. G., and Lin, T. C.: Numerical Methods for Two- and Three-Dimensional Viscous Flow Problems: Application to Hypersonic Leading Edge Equations. Polytechnic Institute of Brooklyn, PIBAL Rep. no. 71-8, April 1971.

8. Cleary, Joseph W.: An Experimental Theoretical Investigation of the Pressure Distribution and Flow Fields of Blunted Cones at Hypersonic Mach Numbers. NASA TN D-2969, 1965.

9. Cleary, Joseph W.: Effects of Angle of Attack and Bluntness on the Shock-Layer Properties of a 15° Cone at a Mach Number of 10.6. NASA TN D-4909, 1968.

10. Cleary, Joseph W.: Effects of Angle of Attack and Bluntness on Laminar Heating-Rate Distributions of a 15° Cone at a Mach Number of 10.6. NASA TN D-5450, 1969.

11. Tannehill, J. C., and Holst, T. L.: Numerical Computation of Two-Dimensional Viscous Blunt Body Flows with an Impinging Shock. AIAA Paper 75-154, presented at AIAA 13th Aerospace Sciences Meeting, Pasadena, Calif., Jan. 20-22, 1975.

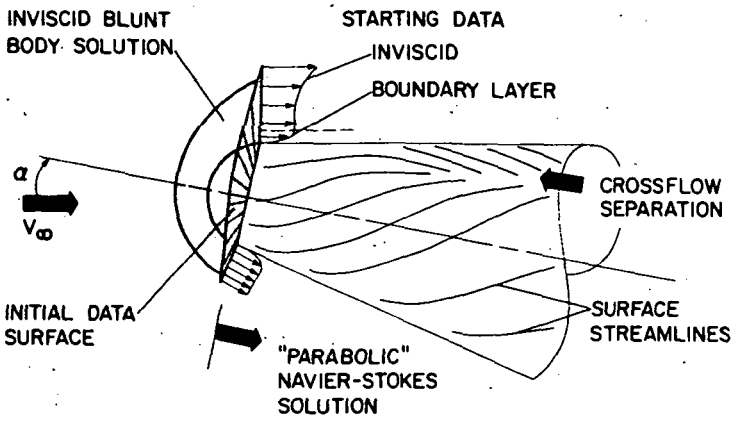

Figure 1.- Laminar viscous vortex flow over a blunt cone.

CALCULATION METHOD:
I VISCOUS IMPLICIT CODE
II INVISCID CHARACTERISTICS CODE

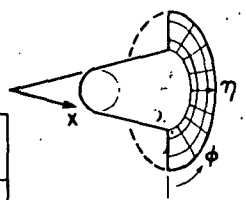

		I VISCOUS	II INVISCID
NUMBER OF MESH POINTS	η	50	21
	ϕ	19	19
	TOTAL	950	399
CDC-7600 COMPUTE TIME (min) $x/R_N = 14.7$	PER STEP	0.26	0.012
	TOTAL	22.9	6.0

Figure 2.- Computational mesh and computer run time.

BLUNT CONE MODEL	
NOSE RADIUS	0.0254 m (1 in.)
CONE HALF-ANGLE	15°
ANGLE OF ATTACK	15°
TEST CONDITIONS (CLEARY)	
MACH NUMBER	10.6
REYNOLDS NUMBER (BASED ON NOSE RADIUS)	1.0×10^5
T_{WALL}/T_{TOTAL}	.26 HEATING TEST 6 PRESSURE TEST

Figure 3.- Conditions for the test case.

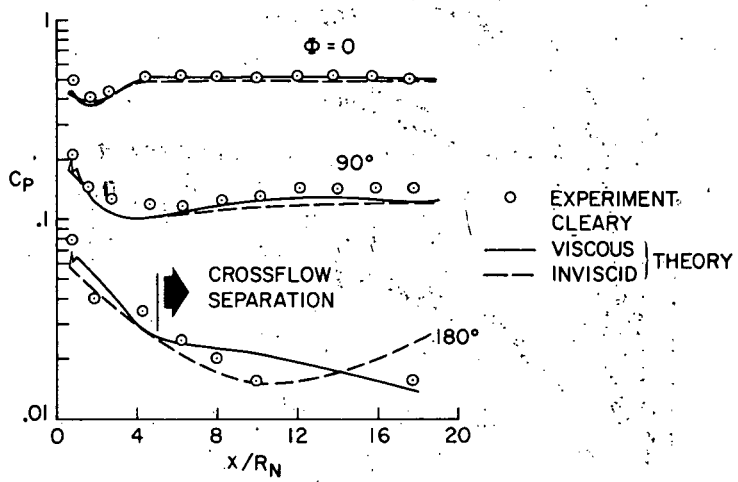

Figure 4.- Surface-pressure coefficient, C_p, for 15° sphere-cone. Angle of attack, 15°; Mach number, 10.6.

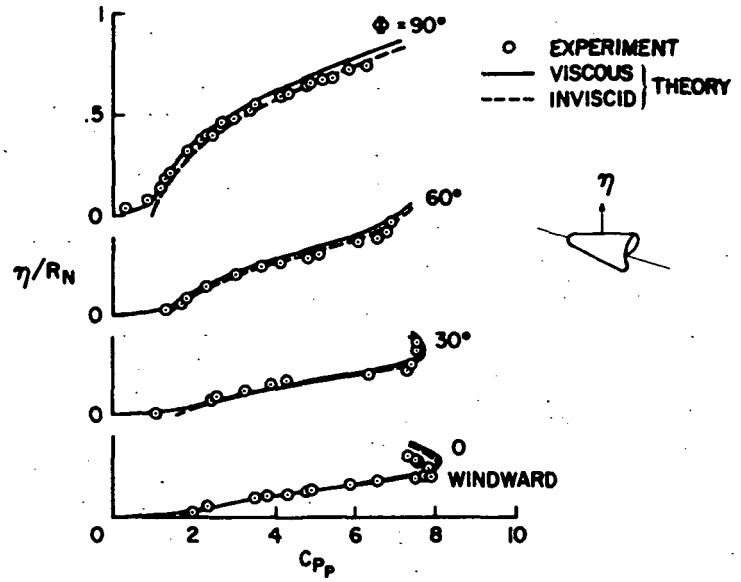

(a) $\Phi = 0° - 90°$.

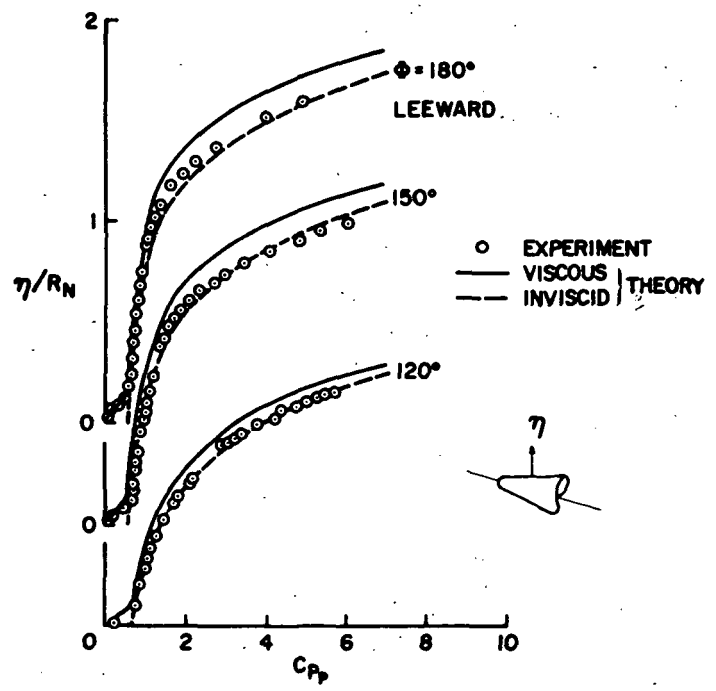

(b) $\Phi = 120° - 180°$.

Figure 5.- Pitot-pressure coefficient, C_{P_p}, across shock layer for 15° sphere-cone. Angle of attack, 15°; Mach number, 10.6; $x/R_N = 3.4$.

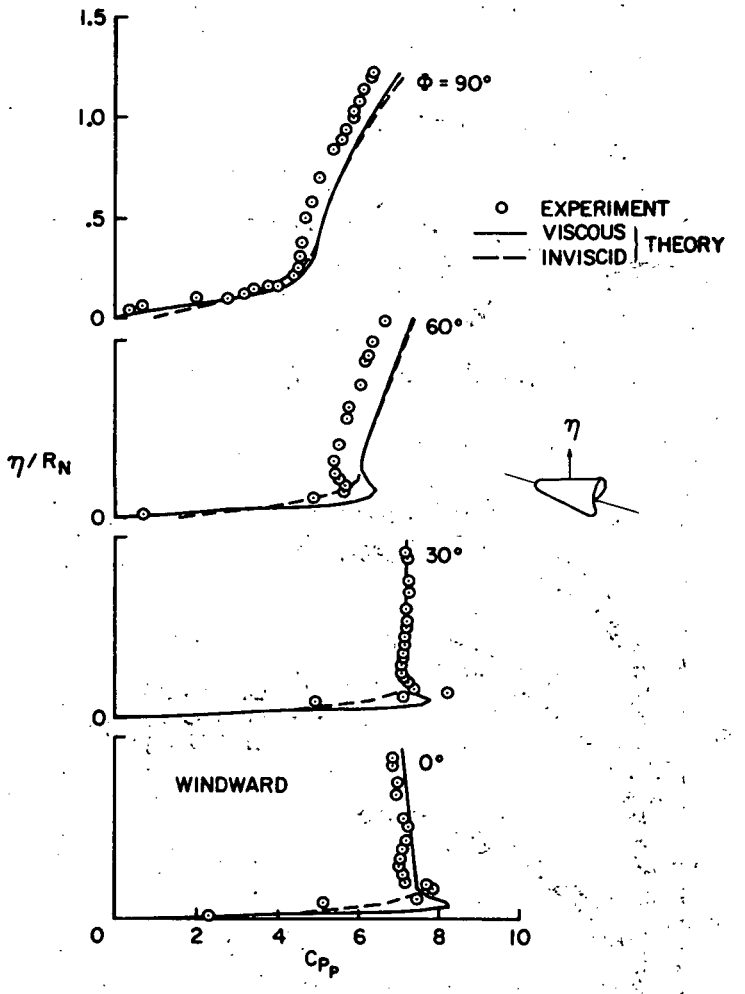

(a) $\Phi = 0° - 90°$.

Figure 6.- Pitot-pressure coefficient, C_{P_p}, across shock layer for 15° sphere-cone. Angle of attack, 15°; Mach number, 10.6; $x/R_N = 14.7$.

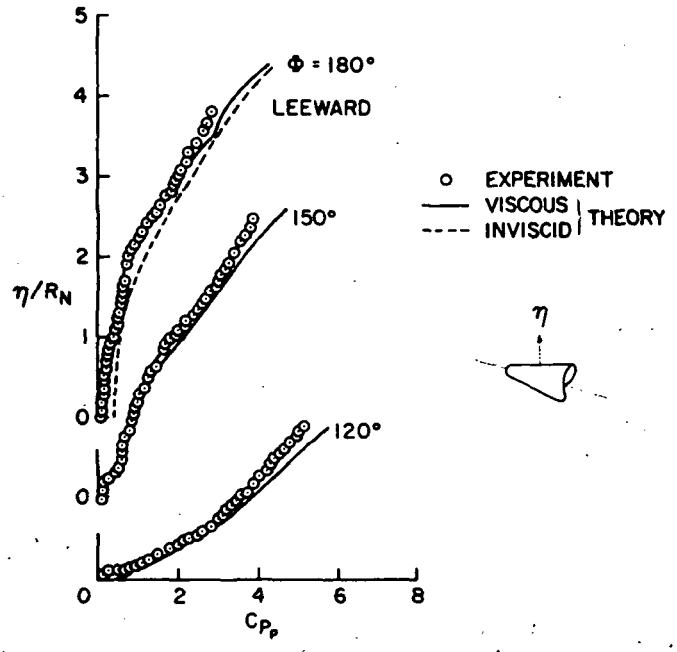

(b) $\Phi = 120° - 180°$.

Figure 6.- Concluded.

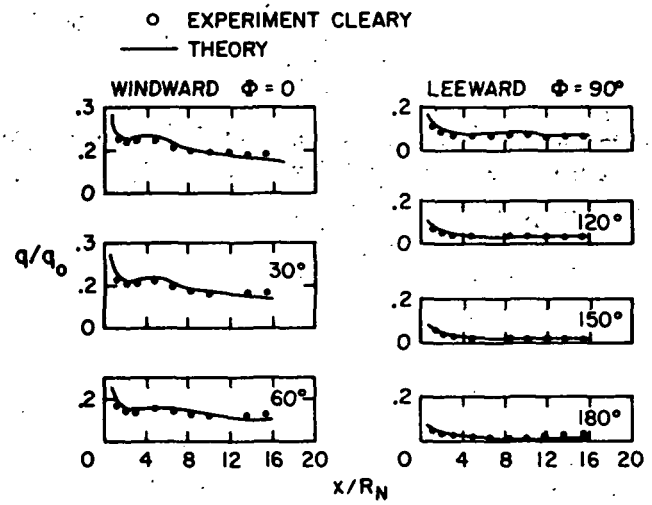

Figure 7.- Surface heating rate ratio, q/q_o, for 15° sphere-cone. Angle of attack, 15°; Mach number, 10.6; $T_{WALL}/T_{TOTAL} = 0.26$; Reynolds number, 1.0×10^5.

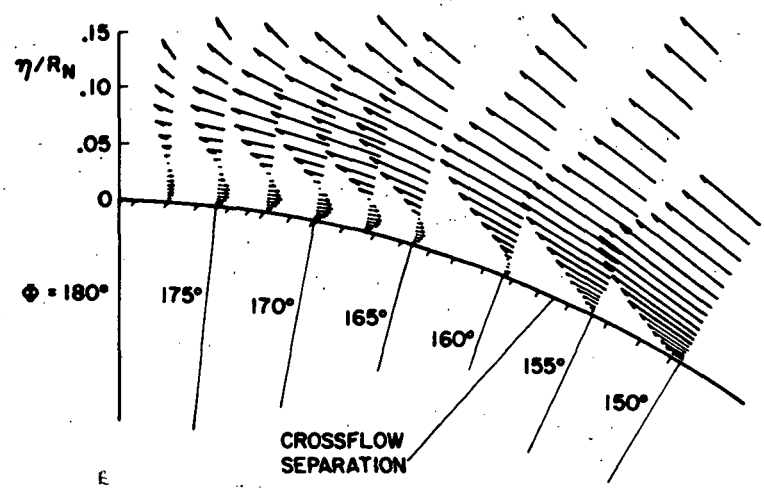

Figure 8.- Crossflow velocity vector field for 15° sphere-cone. Angle of attack, 15°; Mach number, 10.6; $x/R_N = 14.7$; $T_{WALL}/T_{TOTAL} = 0.26$; Reynolds number, 1.0×10^5.